

Doubly-charged Higgs production at lepton colliders within type-II seesaw model

Higgs Potential - Hefei

Shu-Xiang Li

Department of Modern Physics, USTC

December 22, 2024

Outline

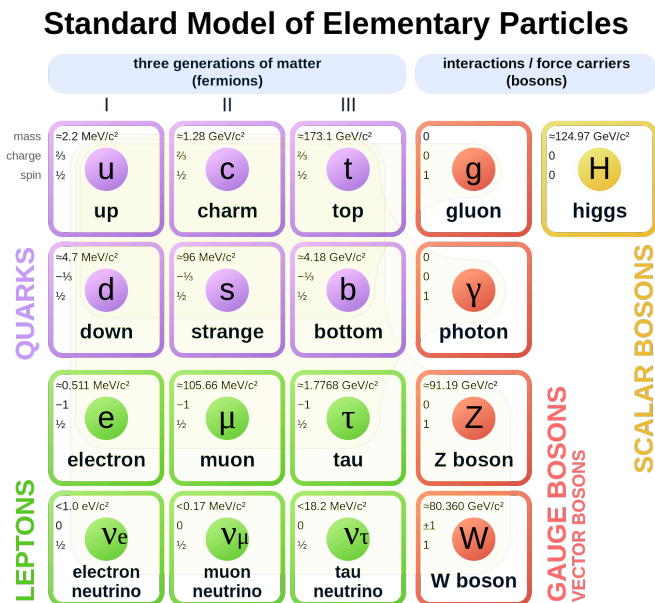
1. Type-II seesaw model
2. Parameter space and production cross section
3. Background analysis
4. Summary

Outline

- 1. Type-II seesaw model**
2. Parameter space and production cross section
3. Background analysis
4. Summary

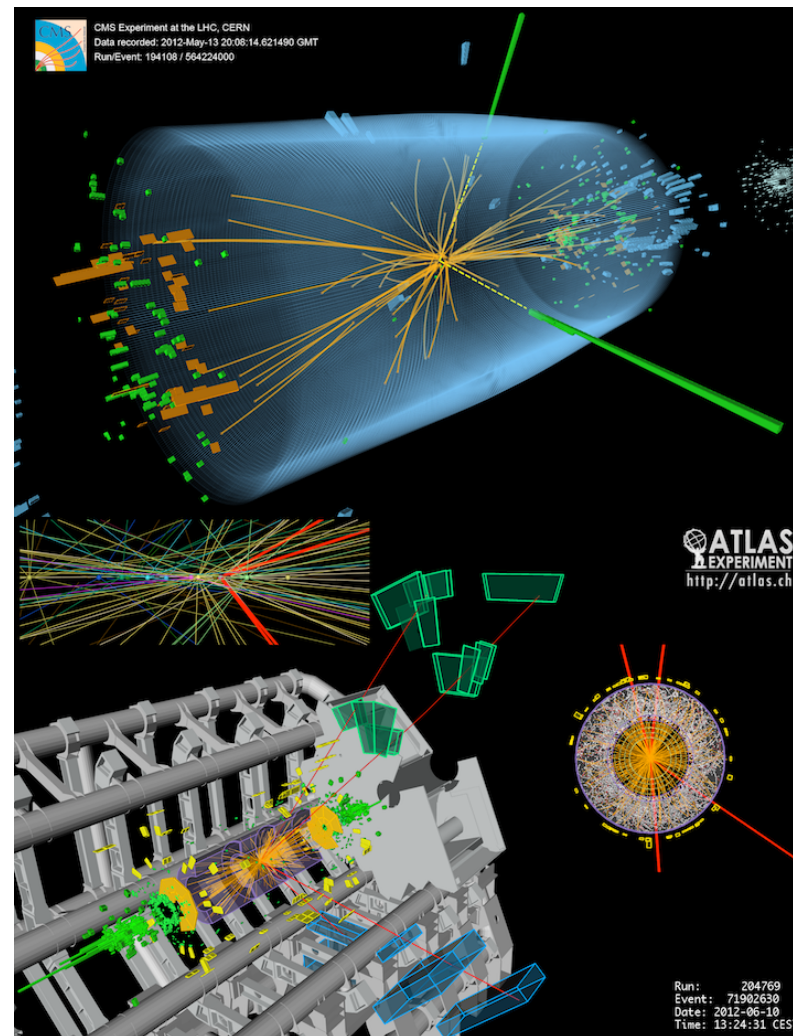
1.1 Beyond the SM

◆ The Standard Model (SM) is **successful**



◆ The SM needs to be **extended**:

- ◆ **neutrino oscillation**
- ◆ dark matter
- ◆ CP violation
- ◆ ...



Candidate Higgs events in ATLAS and CMS

1.2 Seesaw mechanism

Seesaw mechanism is introduced to explain the small masses of neutrinos.

◆ Type-I seesaw:

$$-\mathcal{L}_\nu = Y_D \overline{L}_L \tilde{\Phi} N_R + \frac{1}{2} M_R \overline{N}_R^c N_R + h.c.$$

N_R is a right-handed fermion singlet.

Neutrino mass (with $M_R \gg m_D$):

$$m_\nu = -m_D^T M_R^{-1} m_D$$

◆ **Type-II seesaw:**

$$-\mathcal{L}_\nu = Y_L \overline{L}_L^c i\sigma_2 \Delta L_L + h.c.$$

Δ is a left-handed scalar triplet with vev v_Δ . Neutrino mass:

$$m_\nu = \sqrt{2} Y_L v_\Delta$$

◆ Type-III seesaw:

Introduce a fermion triplet...

1.3 Type II seesaw model

The simplest implementation of the type-II seesaw mechanism.

Adding a SU(2) triplet scalar with hypercharge $Y = 2$ to the SM

$$\Delta = \begin{pmatrix} \frac{\delta^+}{\sqrt{2}} & \delta^{++} \\ \frac{1}{\sqrt{2}}(\delta^0 + i\xi_\Delta + v_\Delta) & -\frac{\delta^+}{\sqrt{2}} \end{pmatrix}$$

The full Lagrangian of the type-II seesaw model:

$$\mathcal{L}_{\text{Type-II}} = \mathcal{L}_{\text{SM}} + \mathcal{L}_\nu + \text{Tr} \left[(D_\mu \Delta)^2 \right] - V_{\Delta, \Phi}$$

The complete **Higgs potential**:

$$\begin{aligned} V_\Phi + V_{\Delta, \Phi} = & -\mu_\Phi^2 (\Phi^\dagger \Phi) + \frac{\lambda}{4} (\Phi^\dagger \Phi)^2 - \mu_\Delta^2 \text{Tr}(\Delta^\dagger \Delta) + \lambda_1 (\Phi^\dagger \Phi) \text{Tr}(\Delta^\dagger \Delta) \\ & + \lambda_2 [\text{Tr}(\Delta^\dagger \Delta)]^2 + \lambda_3 \text{Tr} \left[(\Delta^\dagger \Delta)^2 \right] + \lambda_4 \Phi^\dagger \Delta \Delta^\dagger \Phi \\ & + [\mu \Phi^T i \sigma_2 \Delta^\dagger \Phi + \text{h.c.}] \end{aligned}$$

1.3 Type II seesaw model

The simplest implementation of the type-II seesaw mechanism.

Adding a SU(2) triplet scalar with hypercharge $Y = 2$ to the SM

$$\Delta = \begin{pmatrix} \frac{\delta^+}{\sqrt{2}} & \delta^{++} \\ \frac{1}{\sqrt{2}}(\delta^0 + i\xi_\Delta + v_\Delta) & -\frac{\delta^+}{\sqrt{2}} \end{pmatrix}$$

The full Lagrangian of the type-II seesaw model:

$$\mathcal{L}_{\text{Type-II}} = \mathcal{L}_{\text{SM}} + \mathcal{L}_\nu + \text{Tr} \left[(D_\mu \Delta)^2 \right] - V_{\Delta, \Phi}$$

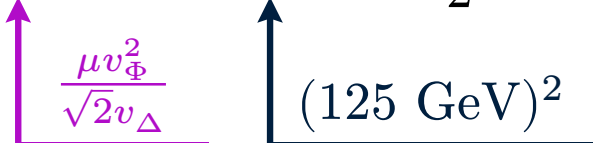
The complete **Higgs potential**:

$$\begin{aligned} V_\Phi + V_{\Delta, \Phi} = & -\mu_\Phi^2 (\Phi^\dagger \Phi) + \frac{\lambda}{4} (\Phi^\dagger \Phi)^2 - \mu_\Delta^2 \text{Tr}(\Delta^\dagger \Delta) + \lambda_1 (\Phi^\dagger \Phi) \text{Tr}(\Delta^\dagger \Delta) \\ & + \lambda_2 [\text{Tr}(\Delta^\dagger \Delta)]^2 + \lambda_3 \text{Tr}[(\Delta^\dagger \Delta)^2] + \lambda_4 \Phi^\dagger \Delta \Delta^\dagger \Phi \\ & + [\mu \Phi^T i \sigma_2 \Delta^\dagger \Phi + \text{h.c.}] \end{aligned}$$

1.3 Type II seesaw model

Mass spectrum of the scalar sector (in the limit $v_\Delta \ll v_\Phi$, see later slide)

$$M_{H^{\pm\pm}} = M_\Delta^2 - \frac{1}{2}\lambda_4 v_\Phi^2, \quad M_{H^\pm} = M_\Delta^2 - \frac{1}{4}\lambda_4 v_\Phi^2,$$

$$M_{A^0}^2 = M_{H^0}^2 = M_\Delta^2, \quad M_{h^0}^2 = \frac{\lambda v_\Phi^2}{2}$$


$v_\Delta, M_{H^{\pm\pm}}, \lambda_{1-4}, Y_L$ as model inputs.

Features of the Type-II seesaw model

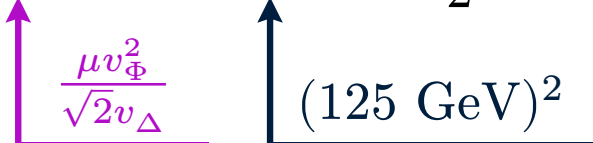
- ◆ neutrino masses
- ◆ doubly-charged Higgs
- ◆ lepton number violation

1.3 Type II seesaw model

Mass spectrum of the scalar sector (in the limit $v_\Delta \ll v_\Phi$, see later slide)

$$M_{H^{\pm\pm}} = M_\Delta^2 - \frac{1}{2}\lambda_4 v_\Phi^2, \quad M_{H^\pm} = M_\Delta^2 - \frac{1}{4}\lambda_4 v_\Phi^2,$$

$$M_{A^0}^2 = M_{H^0}^2 = M_\Delta^2, \quad M_{h^0}^2 = \frac{\lambda v_\Phi^2}{2}$$



$v_\Delta, M_{H^{\pm\pm}}, \lambda_{1-4}, Y_L$ as model inputs.

Features of the Type-II seesaw model

- ◆ neutrino masses
- ◆ doubly-charged Higgs
- ◆ lepton number violation



Outline

1. Type-II seesaw model
- 2. Parameter space and production cross section**
3. Background analysis
4. Summary

2.1 Experimental constraints

- ◆ ρ -parameter: [PDG, 2024]

$$\rho \equiv \frac{m_W^2}{m_Z^2 \cos^2 \theta_W} = \frac{1 + 2v_\Delta^2/v_\Phi^2}{1 + 4v_\Delta^2/v_\Phi^2} = 1.0001 \pm 0.0009$$

$$\downarrow \sqrt{v_\Phi^2 + v_\Delta^2} = 246 \text{ GeV}$$

$$v_\Delta < 4.9 \text{ GeV} \ll v_\Phi$$

- ◆ Direct search

$$M_{H^{\pm\pm}} \quad [\text{ATLAS, 2023}] \quad [\text{ATLAS, 2021}]$$

$$M_{H^{\pm\pm}} > 1065 \text{ GeV}, \quad \text{assuming } \text{Br}(H^{\pm\pm} \rightarrow l^\pm l^\pm) = 100\%$$

$$M_{H^{\pm\pm}} > 350 \text{ GeV}, \quad \text{assuming } \text{Br}(H^{\pm\pm} \rightarrow W^\pm W^\pm) = 100\%$$

$$m_\nu \quad [\text{Planck, 2018}]$$

$$\sum_i m_{\nu_i} < 0.12 \text{ eV}$$

2.1 Experimental constraints

- ◆ Constraints on Y_L ($M_{H^{\pm\pm}} = 1 \text{ TeV}$) [Bhupal, 2018]
 $e^+e^- \rightarrow l^+l^-$

$$|Y_{ee}|^2 < 0.12, \quad |Y_{e\mu}|^2 < 0.064, \quad |Y_{e\tau}|^2 < 0.054$$

muonium oscillation

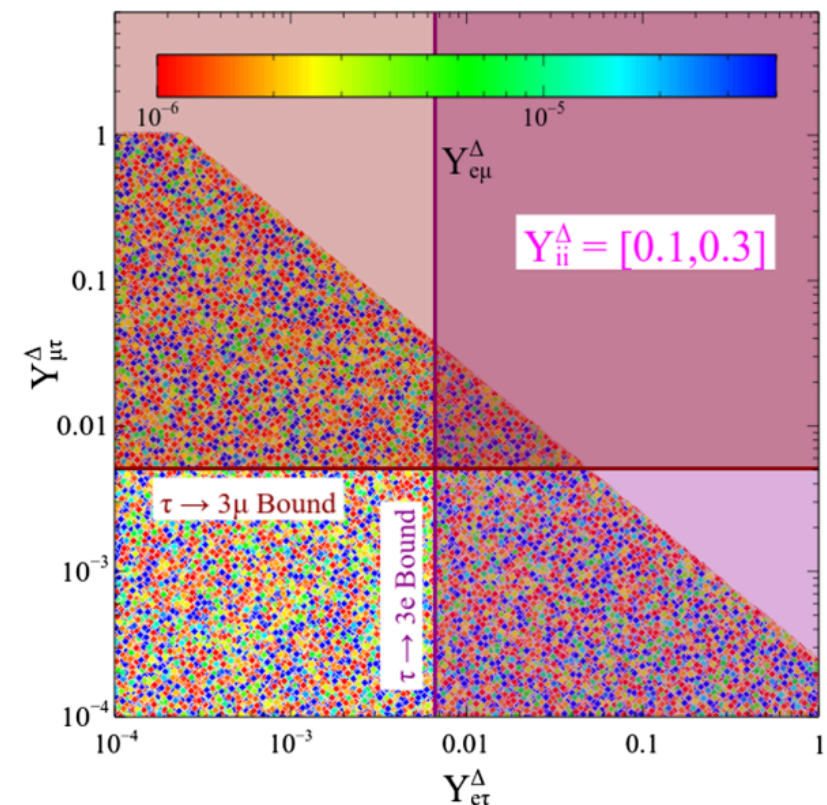
$$|Y_{ee}^\dagger Y_{\mu\mu}| < 0.12$$

lepton flavor violation (LFV)

LFV process	Constraint
$\mu^- \rightarrow e^- e^+ e^-$	$ Y_{ee}^\dagger Y_{e\mu} < 2.3 \times 10^{-5}$
$\tau^- \rightarrow e^- e^+ e^-$	$ Y_{ee}^\dagger Y_{e\tau} < 6.5 \times 10^{-3}$
$\tau^- \rightarrow \mu^- \mu^+ \mu^-$	$ Y_{\mu\mu}^\dagger Y_{\mu\tau} < 6.1 \times 10^{-3}$
...	...

Digonal Y_L are expected to be larger,
 off-diagonal Y_L are highly suppressed.

Allowed off diagonal Yukawa couplings Dev, 2019

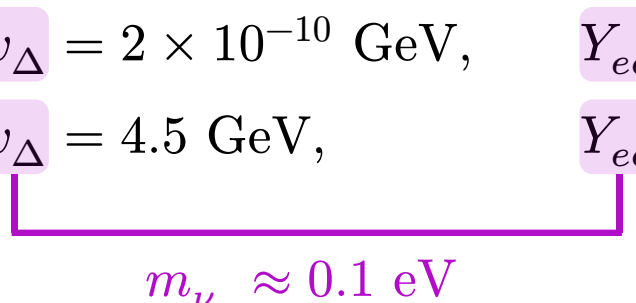


2.2 Parameter setting and benchmark points

$$\lambda_1 = 1, \lambda_2 = \lambda_3 = 0, \lambda_4 = 0.2, Y_{ij} = Y_{ee} \delta_{ie} \delta_{je}$$

Two benchmark points feature a stronger Yukawa coupling and a stronger gauge coupling, respectively.

$$\begin{array}{lll}
 \text{BP1 :} & M_{H^{\pm\pm}} = 1.1 \text{ TeV}, & v_{\Delta} = 2 \times 10^{-10} \text{ GeV}, & Y_{ee} = 0.35 \\
 \text{BP2 :} & M_{H^{\pm\pm}} = 0.4 \text{ TeV}, & v_{\Delta} = 4.5 \text{ GeV}, & Y_{ee} = 1.5 \times 10^{-11}
 \end{array}$$



 $m_{\nu_e} \approx 0.1 \text{ eV}$

The branching ratios at different BPs

$$\text{BP1 :} \quad \text{Br}(H^{\pm\pm} \rightarrow e^{\pm}e^{\pm}) = 100\%$$

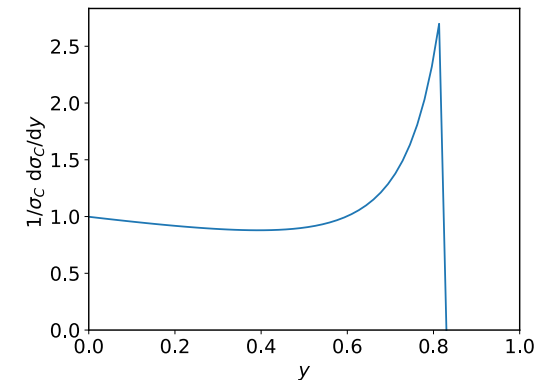
$$\text{BP2 :} \quad \text{Br}(H^{\pm\pm} \rightarrow W^{\pm}W^{\pm}) = 100\%$$

2.3 Production at lepton colliders

Lepton colliders with energy above our benchmark $M_{H^{\pm\pm}}$

	ILC	CLIC phase II	CLIC phase III
\sqrt{s} (TeV)	1.0	1.5	3.0
\mathcal{L} (ab) ⁻¹	2.0	2.5	5.0

Photon energy spectrum at $x = 4.5$



Consider 4 collision modes:

$$e^+e^- \quad e^-e^- \quad e^-\gamma \quad \gamma\gamma$$

Photon beam from Compton scattering

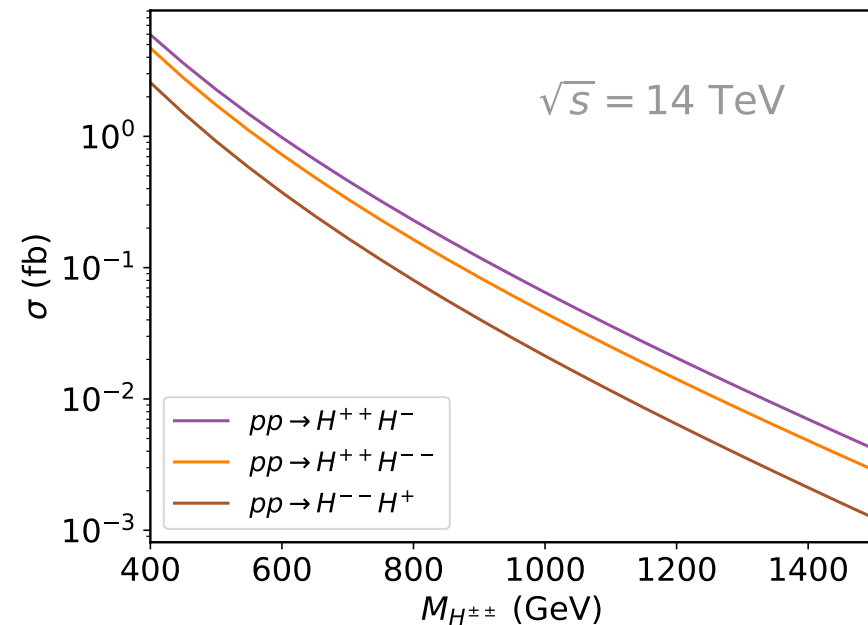
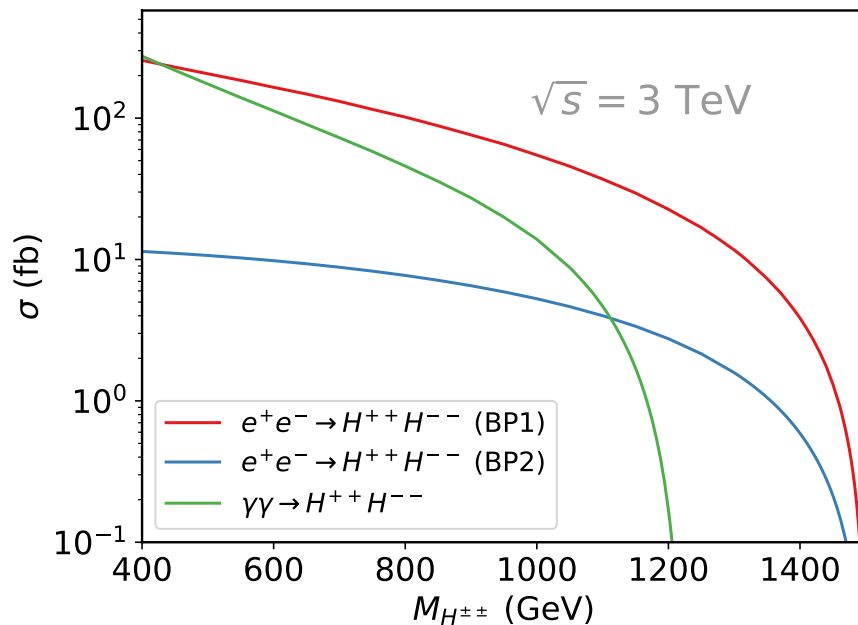
$$y_{\max} = 0.83$$

$$\frac{1}{\sigma_C} \frac{d\sigma_C}{dy} = \left[1 - y + \frac{1}{1-y} - \frac{4y}{x(1-y)} + \frac{4y^2}{x^2(1-y)^2} \right] / (\ln x + 1/2)$$

ω_γ/E_e

$4E_e\omega_0/m_e^2 = 4.5$

2.4 Pair production cross section

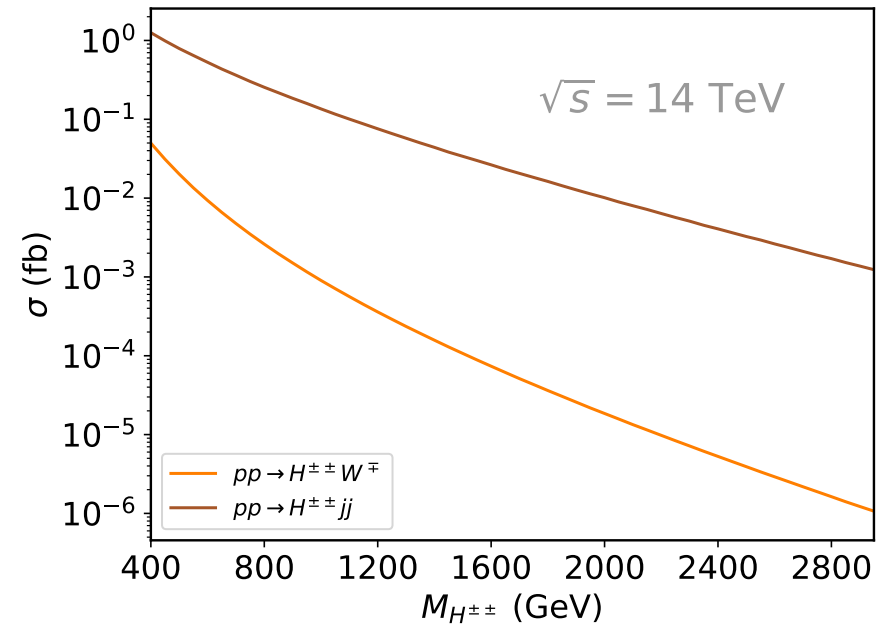
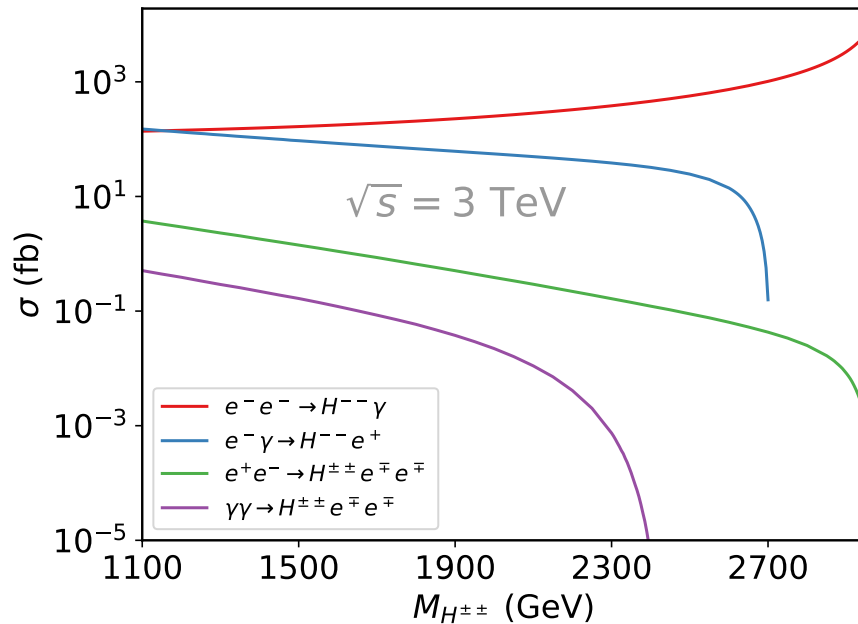


Pair production at lepton and pp colliders.

- ◆ **e^+e^- mode** The t -channel exchange of $H^{\pm\pm}$ contributes significantly at large Yukawa coupling (BP1).
- ◆ **$\gamma\gamma$ mode** threshold effect: $y_{\max} \times \sqrt{s}/2 \approx 1200 \text{ GeV}$.
- ◆ **pp collider** smaller compared lepton colliders.

2.5 Single production cross section

The dominant single production processes at BP1 (left) and BP2 (right)



- ◆ **lepton collider** dominates with larger Yukawa coupling
- ◆ **pp collider** benefits from stronger gauge coupling
- ◆ **e^-e^- mode** largest cross section, increase due to $\frac{1}{s-M_{H^{\pm\pm}}^2}$

Outline

1. Type-II seesaw model
2. Parameter space and production cross section
- 3. Background analysis**
4. Summary

3.1 Pair production background - pp

Take pair production at pp collider as a demonstration of our background analysis.

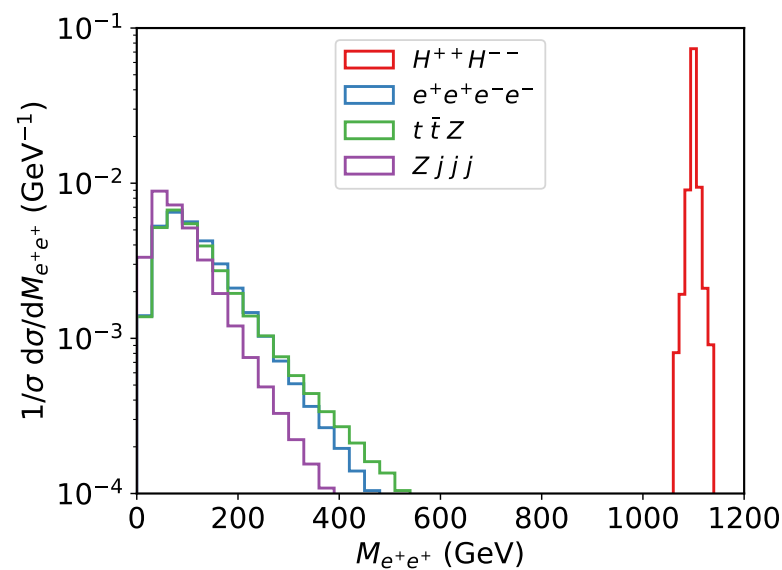
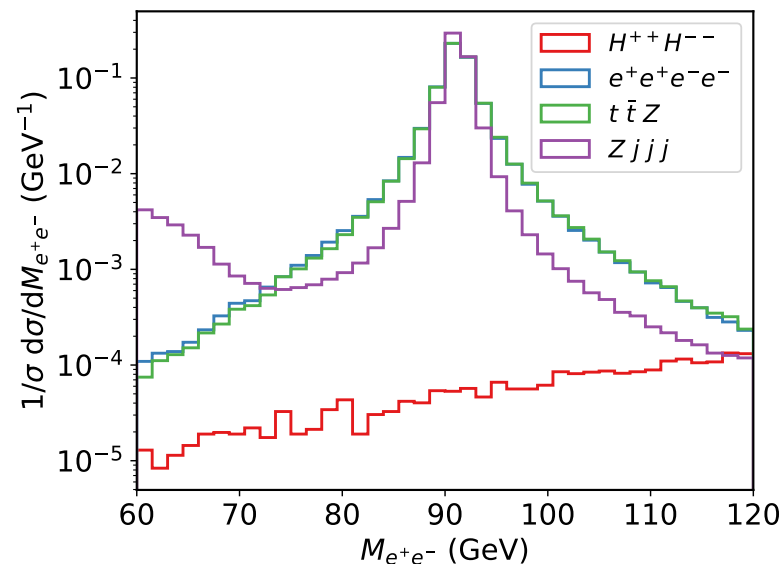
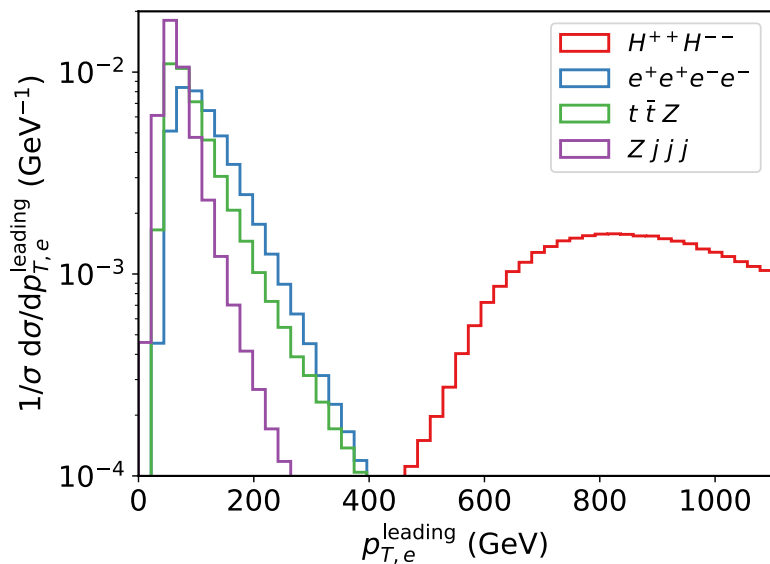
Cross sections of $H^{++}H^{--}$ and dominant background processes ($\sqrt{s} = 14$ TeV).

Process	σ (pb)	Decay channel	σ' (fb)
$H^{++}H^{--}$	2.50×10^{-5}	$e^+e^+ + e^-e^-$	0.0219
$e^+e^+e^-e^-$	0.00648		6.48
$t\bar{t}Z$	0.693	$e^+\nu_e b + e^-\bar{\nu}_e \bar{b} + e^+e^-$	0.181
$Zjjj$	2.33×10^3	e^+e^-	0.167

σ' is obtained by multiplying the branching ratio and applying the baseline cut (selection):

$$p_T(e) > 10 \text{ GeV}, \quad |\eta(e)| < 2.5, \quad \Delta R(e, e) > 0.4$$

3.1 Pair production background - pp



Normalized distribution for
 $p_{T,e}^{\text{leading}}$, $M_{e^+e^-}$ and $M_{e^+e^+}$

3.1 Pair production background - pp

Number of events after cut ($\mathcal{L} = 300 \text{ fb}^{-1}$)

Process	Baseline cut	$p_{T,e}^{\text{leading}}$	$M_{e^+e^-}$	$M_{e^\pm e^\pm}$
$H^{++}H^{--}$	6.58	6.44	6.42	6.42
$e^-e^-e^+e^-$	1.94×10^3	0.27	0.0311	0
$t\bar{t}Z$	54.4	0.0673	7.05×10^{-4}	0
$Zjjj$	50.2	0.109	0.00115	0

Cuts flow:

1. $p_{T,e}^{\text{leading}}$

$$p_{T,e}^{\text{leading}} > M_{H^{++}}/2$$

Signal significance:

$$\mathcal{S} = 2.54$$

2. $M_{e^+e^-}$

$$\forall (e^+, e^-) \quad |M_{e^+e^-} - M_Z| > 10 \text{ GeV}$$

3. $M_{e^\pm e^\pm}$

$$|M_{e^\pm e^\pm} - M_{H^{++}}| < 0.1 \times M_{H^{++}}$$

3.2 Single production background - e^-e^-

Cross sections of $H^{--}\gamma$ and dominant background processes ($\sqrt{s} = 3.0$ TeV).

Process	σ (fb)	Decay channel	σ' (fb)
$H^{--}\gamma$	138	e^-e^-	138
$e^-e^-\gamma$	199		199
$e^-\nu_e W^-\gamma$	89.9	$e^-\bar{\nu}_e$	9.63
$e^-e^-\gamma\gamma$	5.25		0.525
$\nu_e\nu_e W^-W^-\gamma$	5.66	$e^-\bar{\nu}_e + e^-\bar{\nu}_e$	0.0649

Number of events after cut ($\mathcal{L} = 300 \text{ fb}^{-1}$). $\mathcal{S} = 173.7$

Process	Baseline cut	$p_{T,e}^{\text{leading}}$	$M_{e^-e^-}$
$H^{--}\gamma$	3.88×10^4	3.02×10^4	3.02×10^4
$e^-e^-\gamma$	5.96×10^3	2.42×10^3	38.7
$e^-\nu_e W^-\gamma$	224	40.3	4.68
$e^-e^-\gamma\gamma$	15.7	8.64	0.304
$\nu_e\nu_e W^-W^-\gamma$	1.67	0.0672	0.00759

3.3 Significance

Signal significance for pair production in different modes at BP1

$M_{H^{\pm\pm}}$	1100	1250	1400
e^+e^-	97	64	29
$\gamma\gamma$	31	/	/

The 5σ sensitivity reach of Y_{ee} for single production at BP1.

$M_{H^{\pm\pm}}$	1100	1500	1900	2300	2700
e^-e^-	0.022	0.022	0.021	0.020	0.020
$e^-\gamma$	0.019	0.023	0.029	0.040	1.5
e^+e^-	0.068	0.12	0.22	0.43	1.1
$\gamma\gamma$	0.21	0.43	1.1	12	/

Outline

1. Type-II seesaw model
2. Parameter space and production cross section
3. Background analysis
4. **Summary**

4.1 Summary

- ◆ Consider four collision modes at 3 TeV CLIC
- ◆ Compare the **pair** and **single** production $H^{\pm\pm}$ with 14 TeV LHC
- ◆ Pair production signals are **much more significant** at CLIC
- ◆ Yukawa coupling at **two hundredths** level \Rightarrow doubly charged Higgs discovery

4.1 Summary

- ◆ Consider four collision modes at 3 TeV CLIC
- ◆ Compare the **pair** and **single** production $H^{\pm\pm}$ with 14 TeV LHC
- ◆ Pair production signals are **much more significant** at CLIC
- ◆ Yukawa coupling at **two hundredths** level \Rightarrow doubly charged Higgs discovery

Thanks!